On the Generality and Strength of Transition Metal β-effects

Brandon E. Haines, Richmond Sarpong, Djamaladdin G. Musaev*

Cherry L. Emerson Center for Scientific Computation, Emory University, Atlanta, Georgia 30322, United States
Department of Chemistry, University of California, Berkeley, California 94720, United States

Supporting Information Placeholder

Abstract. Using computation, we examine the generality and strength of β-effects from transition metal centers on β-elimination. In particular, we find that a β-Pd(II) substituent imparts over twice the stabilization to a carbocation as a Si substituent, representative of the well-known β-silicon effect. We established efficient and practical computational parameters to investigate the σσ conjugation in an experimentally relevant system: *N,N*-picolinamide vinyl metalacycles with β-substituents that can undergo elimination. We have found that the β-Pd effect depends on the nature of the C_β substituent (X): This effect is negligible for X = H, Me, OH and F, but is significant for X = Cl, Br and I. We have also extended these studies to the β-effect in *N,N*-picolinamide vinyl metalacycles with β-substituents of other transition metals—Fe(II), Ru(II), Os(II), Co(III), Rh(III), Ir(III), Ni(II), Pd(II), Pt(II), Cu(III), Ag(III), and Au(III). We found that the electronegativity of the metals correlates reasonably well with the relative β-effects, with first-row transition metals exerting the strongest influence. Overall, it is our anticipation that a more profound appreciation of transition metal β-effects will facilitate the design of novel reactions, including new variants of transition metal catalyzed C–H functionalization.

Introduction

Hyperconjugative interactions—defined as stereoelectronic interactions involving at least one σ orbital—are ubiquitous in chemistry and have profound effects on reactivity and conformational equilibria.[1-3] A prominent example is the β-effect of silicon (or β-Si effect), where a R_3Si substituent stabilizes positive charge at a position β to the silicon group, manifesting extraordinary rate accelerations,[4-7] activation of typically inert functionalities[8-9] (e.g., C–H bonds[10]), control over selectivity,[11-13] and the isolation of typically high energy carbocation[14-18] and carbene[19-20] species.

The β-Si effect is generally attributed to hyperconjugation (also called σπ conjugation) through the interaction between a Si–C_α σ orbital and the empty π-orbital of a carbocation centered on C_β (Figure 1A).[21-25] Other atoms with an empty orbital, such as boron, can engage in this type of hyperconjugation.[26] This effect has also been evoked in considering hyperconjugation between a Si–C_α σ orbital and an empty σ* orbital of a C_β–X bond (also called σσ conjugation, Figure 1B).[27-32] It should be noted that hyperconjugation is not the only factor that contributes to the β-Si effect. Most notably, neighboring group participation, whereby the β-Si migrates to stabilize the positive charge through a bonding interaction, has also been proposed as a mechanism that rationalizes the β-Si effect (Figure 1C).[33-36]

In general, the Si–C σ–bond has several qualities that are well-suited to hyperconjugation: It is polarizable, matches the energy of the acceptor orbital, and Si is electropositive enough to accept the positive charge resulting from delocalization. Extensive studies on varying the substituents on Si,[37] using other group 14 metals (e.g., Ge, Sn and Pb),[38-39] almost all second and third period elements,[40-41], fourth period main group elements,[42] as well as various phosphorous groups[43] and sulfonyls,[44] have established electronegativity as a strong indicator of σ-donor ability in connection with β-effects.

On this basis, Lambert hypothesized that transition metals should also be well-suited to exhibiting β-effects.[22] Consistent with this hypothesis, we recently reported the "β-Pd effect" as part of a mechanistic study of the regiodivergence in a Pd(II)-catalyzed C–H alkynylation reaction.[45-46] There, we showed that hyperconjugation between the Pd–C_α σ donor orbital and acceptor σ* orbital of a C_β–Br bond (i.e., σσ conjugation) facilitates vinyl β-bromide elimination to form an alkyne (Figure 1D).[46] However, there are limited examples of transition metal hyperconjugative β-effects proposed in the literature. Notably, it was shown that the stabilization of a carbocation from a β-Au substituent switches the Bergman cyclization from a diradical mechanism to a zwitter-ionic mechanism and makes it a thermodynamically favorable reaction.[47] Additional examples include cobalt carbonyl cluster complexes,[48] metallocenes,[49] and mercury.[25, 50] Invoking this effect for Pd and other transition metals generally employed in catalysis has significant implications.

1A. Role of □□ conjugation in the □-Si effect:

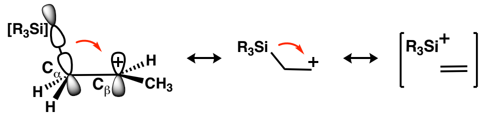

1B. Role of □□ conjugation in the □-Si effect:

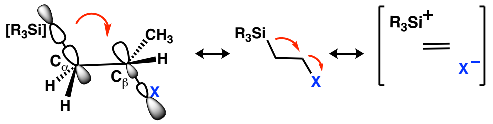

1C. Neighboring group participation in the □-Si effect:

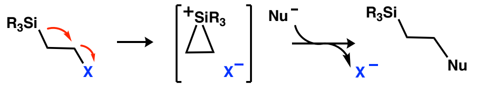

1D. Proposed □-Pd effect, ref. 44

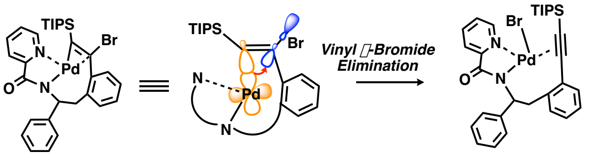

1E. *This Work*

Generality and Trends of □□ conjugation in the □-effect for Transition Metals

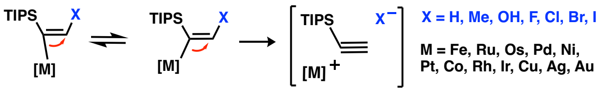

Figure 1. Summary of the β-Si effect and its extension to transition metals. Here, [M] stands for the *N*,*N*-picolinamide vinyl metalacycles with β-substituents of metal M.

One likely reason for the limited examples of β-transition metal effects is the instability of transition metal alkyl and vinyl intermediates under typical experimental conditions. However, computation can be used to study the properties and reactivity of these high energy intermediates. Here, we use modern computational methods, including density functional theory calculations, to establish a theoretical framework and interrogate trends for transition metal β-effects (Figure 1E). Overall, it is our anticipation that a more profound appreciation of transition metal β-effects would facilitate the design of novel reactions, including various types of catalytic C–H functionalization.

Results and Discussion

As a starting point, we constructed a model system to demonstrate the aforementioned σπ and σσ conjugation and to establish the primary computational parameters used here to quantify these effects. (See the Supporting Information for more details.) We also use these model systems to compare the β-effects arising from Pd(II) and Si substituents using models [M] = $PdCl(NH_3)_2$ and SiH_3[40-41, 51-53], respectively (Figure 2).

2A. σπ-conjugation and inductive interactions between the [M] donor group and empty π-acceptor orbitals of the C_β-center of the model system $[M]CH_2CH^+CH_3$.

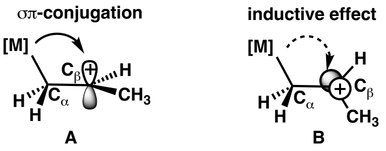

2B. σσ-conjugation between the [M] donor group and σ* acceptor orbital of the C_β-center of the model system $[M]CH_2CHBrCH_3$.

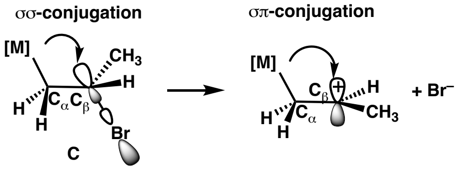

Figure 2. Schematic presentation of the σπ and σσ conjugations and inductive effect in the model systems $[M]CH_2CH^+CH_3$ and $[M]CH_2CHBrCH_3$, respectively, where [M] = SiH_3 and $PdCl(NH_3)_2$.

As mentioned above, traditionally, the β-Si effect is attributed to the σπ conjugation involving the interaction of the Si-C_α σ donor orbital and acceptor π-orbital of a carbocation centered on C_β (Figures 1A and 2A).[21-25] Thus, the stabilization arising from σπ conjugation from a substituent [M] relative to H can be quantified using the isodesmic reaction in equation 1.

$$CH_3CH_2CH_3 + [M]CH_2CH^+CH_3\ (\mathbf{A}/\mathbf{B}) \rightarrow$$
$$[M]CH_2CH_2CH_3 + CH_3CH^+CH_3 \qquad (1)$$

To distinguish between the stabilization of the carbocation due to hyperconjugation and non-directional inductive effects for [M] = SiH_3 and $PdCl(NH_3)_2$, we calculated two rotational isomers for the cation

$[M]CH_2CH^+CH_3$ as described in the literature[40-41, 51-53]: In its bisecting isomer (**A**), the [M] substituent is parallel with the empty orbital of the cationic center to form ideal hyperconjugative interactions. In the eclipsing isomer (**B**), the [M] substituent is perpendicular to the empty orbital of the cationic center so that it is impossible to form hyperconjugative interactions and any stabilization arises only from non-directional inductive effects (Figure 2A). The difference in stabilization energy (ΔE from Eq. 1) between these isomers (i.e., $\Delta\Delta E_{AB} = \Delta E_A - \Delta E_B$) provides a measure of the stabilization from the σπ hyperconjugation.

For [M] = SiH_3, we compute 18.0 kcal/mol stabilization from σπ hyperconjugation which is consistent with previous studies.[40-41, 51-53] For [M] = $PdCl(NH_3)_2$, we compute 44.2 kcal/mol stabilization indicating that the Pd(II) ion can provide over twice as much stabilization through hyperconjugation as Si. (See the Supporting Information for more details.) This trend is consistent with computations using other electropositive β-substituents.[40-41]

With this understanding, it is reasonable that introduction of an electronically diverse range of X substituents at the C_β-center may perturb the nature of the β-effect by changing the acceptor orbital from an empty π-orbital of the carbocation to a σ* orbital of the C_β–X bond. As a result, the interaction between the [M]–C_α σ donor orbital and σ* acceptor orbital of C_β–X bond becomes the major contributor to the β-effect. This type of conjugation is termed σσ conjugation.[27-32]

To quantify σσ conjugation, we adjusted the model system to $[M]CH_2CHXCH_3$, where X = Br (**C** in Figure 2B). In this model, we expect that σσ conjugation will lead to C_β–Br bond elongation relative to 2-bromopropane (i.e., [M] = H), where D(C_β–Br) = 2.09 Å. To test this hypothesis, we calculated ΔD(C_β–Br) in **C** for [M] = $PdCl(NH_3)_2$ and SiH_3. This change in bond distance is found to be 0.12 Å and 0.03 Å, for [M] = $PdCl(NH_3)_2$ and SiH_3, respectively. Thus, the degree of C_β–Br bond elongation, i.e. ΔD(C_β–Br), can be used as an effective parameter for quantifying the σσ conjugation as part of the β-effect These data again show that the β-Pd(II) effect is substantially larger than the β-Si effect.

In order to obtain additional support for this conclusion, we also used natural bond orbital (NBO) analysis to compute the extent of delocalization of electrons between the occupied [M]–C_α σ orbital and the empty C_β–Br σ* orbital. Here, we used the second-order perturbation energy, $E^{(2)}_{ij}$, calculated from the Fock matrix element, F_{ij}, and the energy gap, ΔE, for the interacting donor (i) and acceptor (j) orbitals.[54] Consistent with the calculated change in C_β–Br bond distance in **C**, we find a smaller $E^{(2)}_{ij}$ value for [M] = SiH_3 than for $PdCl(NH_3)_2$: 8.0 and 20.9 kcal/mol, respectively.[55] (See the Supporting Information for more details.) Thus, these model studies consistently show that the β-Pd(II) substituent is over twice as stabilizing towards positive charge as a β-Si group either through σπ or σσ conjugation.

These model studies also justify our use of σσ conjugation to more broadly study β-transition metal effects. Using σσ conjugation is desirable because the reactant complexes for substitution or elimination reactions (i.e., with a C_β–X σ bond) are more computationally tractable than high energy carbocations. Furthermore, practical computational parameters that have been identified above: a) the change in C_β–X bond distance relative to a suitable reference structure, ΔD(C_β–Br) and b) the second-order perturbation energy, $E^{(2)}_{ij}$, can be employed to quantify β-effect of various transition metals. Thus, this approach is more effective and convenient. On the basis of the results above, we expect that the magnitude of the σπ conjugation will remain significant, but the computed trends from σσ conjugation will be valid and helpful for design of novel transition metal catalysis.

We next turned to a specific system to further investigate the potential and scope for transition metal β-effects arising from σσ conjugation: Pd(II)-mediated site-selective $C(sp^2)$–H alkynylation of substrates with β-carbolinamide and picolinamide as *N,N*-bidentate chelating groups using TIPS-alkyne-halide coupling partners (see Figure 3, π-complex structure **1**). We previously showed that the reaction using TIPS-alkyne-bromide proceeds through migratory insertion transition state **TS1** and leads to the formation of a Pd-alkenyl intermediate with a β-bromide substituent.[46] This intermediate has two isomeric forms, **2** and **3**, which we term “constrained” and “relaxed” geometry intermediates, respectively.

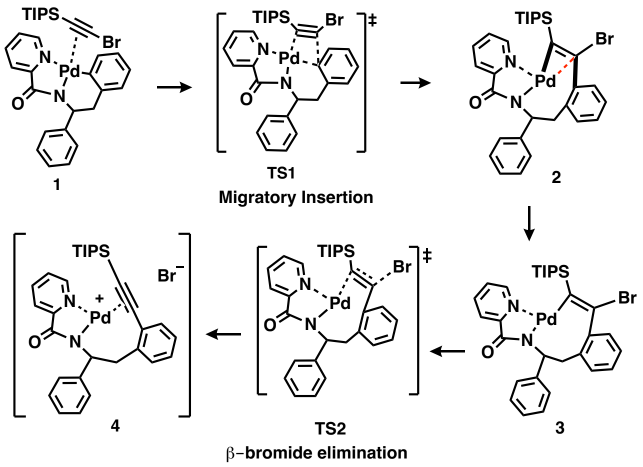

Figure 3. Mechanism for Pd(II)-mediated site-selective C(sp^2)–H alkynylation of substrates with β-carbolinamide and picolinamide as *N,N*-bidentate chelating groups using TIPS-alkyne-bromide coupling partners

We found that the direct product of the migratory insertion transition state (see **TS1**) is a "constrained" geometry structure (**2**) where the double bond is involved in direct interactions with the Pd. Interestingly, this structure resembles an intermediate expected via the neighboring-group mechanism (Figure 1C). However, in this Pd-alkenyl intermediate, hyperconjugation, which is initiated in **TS1**, is clearly also present: The *trans* σ(Pd–C_α) and σ*(C_β–Br) orbitals are strongly interacting ($E^{(2)}_{ij}$ = 28.1 kcal/mol) and the C_β–Br bond is significantly elongated (ΔD(C_β–Br) = 0.09 Å). However, structure **2** is ΔG = 15.6 kcal/mol less stable than the "relaxed" geometry intermediate **3**. The computed hyperconjugation parameters of **3**, $E^{(2)}_{ij}$ = 28.5 kcal/mol and ΔD(C_β–Br) = 0.10 Å, are very similar to those of **2**. For Pd(II), this indicates that the hyperconjugation is the dominant factor in the β-effect regardless of the possible interactions between the metal d orbitals and the alkene π orbitals. Then, from **3**, the established β-Pd effect enables elimination of the vinyl β-bromide via transition state **TS2** with a small free energy barrier ($\Delta G^{\ddagger}_{\text{elim}}$ = 3.6 kcal/mol). Of note, prior to our study, additives[56-58] or a β-silicon substituent[22] was thought to be necessary to facilitate this step.

Close analysis of the electronic structure of Pd-alkenyl intermediate **3** reveals the existence of complex donor-acceptor interactions between the alkene and Pd. In this intermediate, the σ(Pd–C1) and σ*(Pd–C1) orbitals interact with the $\pi_x(C_\beta\equiv C_\alpha)$ and combined $\lambda^* = c_1\sigma^*(C_\beta–X) + c_2\pi_x^*(C_\beta\equiv C_\alpha)$ orbitals to form new σ(C1–C_β) and Pd–C_α/alkene σ/π bonds (Figure 4).

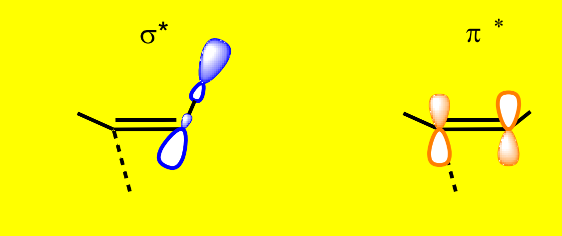

Figure 4. The alkyne orbitals that mix to form the hybrid orbitals, λ* (see Figure 5).

For X = Me, the σ*(C_β–X) orbital is higher in energy than the anti-bonding π_x^*-orbital of $C_\beta\equiv C_\alpha$, so it contributes less to the hybrid λ* orbital (termed λ_π*) and, consequently, to the Pd-alkene interaction, which makes the hyperconjugation weaker. (Figure 5) Indeed, for the interaction between the σ(Pd–C) orbital and the σ*(C–CH_3), $E^{(2)}_{ij}$ = 8.2 kcal/mol in complex **3**. However, as the σ*(C_β–X) orbital becomes lower in energy, its involvement in the λ* orbital becomes larger (termed λ_σ*), and, consequently, the hyperconjugation is enhanced. (Figure 5) For example, for X = Br, the σ*(C_β–Br) orbital is more stable than the $\pi_x^*(C_\beta\equiv C_\alpha)$ orbital [*i.e.* σ*(C_β–X) to $\pi_x^*(C_\beta\equiv C_\alpha)$ where an orbital switch has occurred!]. This results in a stronger interaction of the σ*(C_β–Br) orbital with the σ (Pd–C_α) orbital.

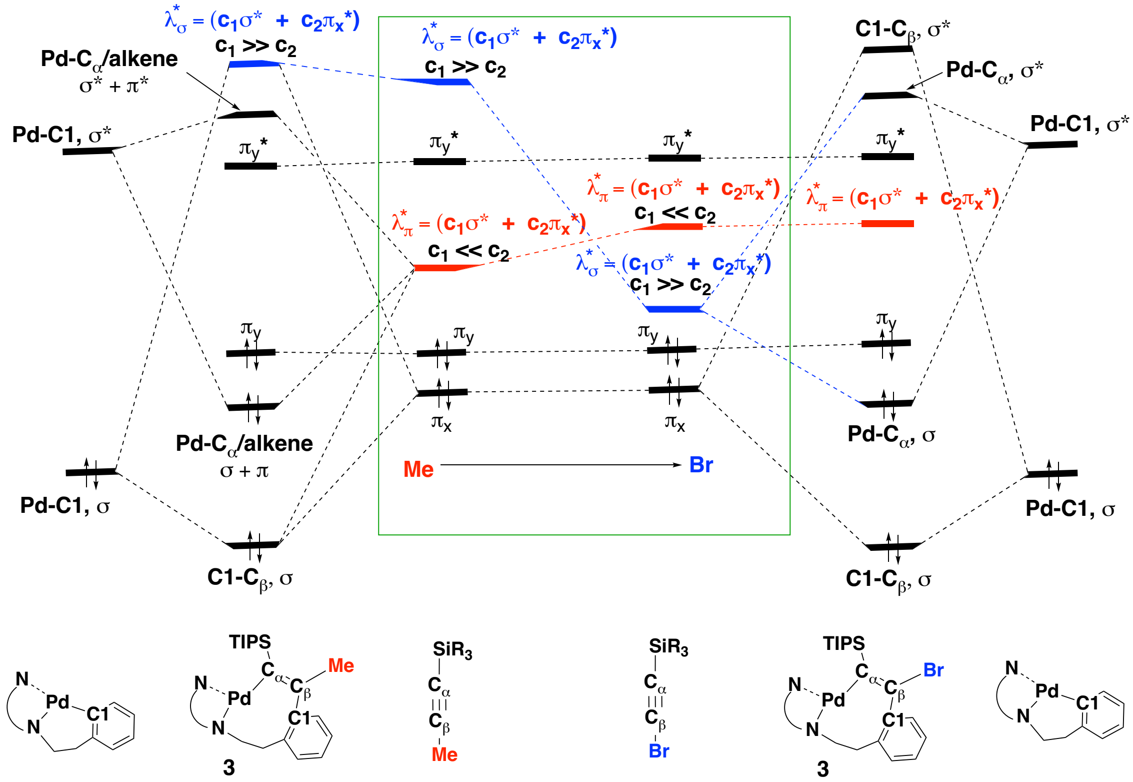

Figure 5. Molecular orbital diagrams for the formation of Pd-alkenyl complexes with TIPS-alkyne-X, where X = Me and Br.

Table 1. Hyperconjugation parameters for Pd-alkenyl intermediate **3** with different X substituents.

X =	$\Delta D(C_\beta$ –X) Å	$E^{(2)}_{ij}$ kcal/mol	ΔE a.u.	F_{ij} au	$\Delta G^\ddagger_{elim}$ kcal/mol
H	0.00	6.5	0.87	0.067	N/A
CH_3	0.00	8.2	0.79	0.072	N/A
OH	0.00	12.1	0.68	0.085	> 50*
F	0.01	15.5	0.58	0.088	> 40*
Cl	0.07	25.0	0.41	0.093	7.5
Br	0.10	28.5	0.36	0.092	3.6
I	0.11	27.5	0.33	0.088	1.0

*Values estimated from relaxed potential energy scan of the C_β–X distance. (See the Supporting Information)

Armed with this fundamental insight, we next sought to assess the generality and define trends for transition metal β-effects using our established computational tools: (a) change in C_β–X bond distance in **3** relative to a reference alkene Ph(X)C=CH(TIPS), where X and TIPS are in a *cis* relationship, $\Delta D(C_\beta–X)$, (b) interaction energy between the participating orbitals, $E^{(2)}_{ij}$, along with F_{ij} and ΔE, and, where possible, (c) the free energy barrier for β-elimination of the X group, $\Delta G^\ddagger_{elim}$.

Trends in transition metal β-effects: Impact of the X substituent at C_β. The hyperconjugation parameters for **3** with X = H, Me, OH, F, Cl, Br, and I, and M = Pd(II) are shown in Table 1. (The values computed for **2** are consistent. See the Supporting Information.) The computed values for $\Delta D(C_\beta–X)$, $E^{(2)}_{ij}$ (including F_{ij} and ΔE, where *i* and *j* stand for the σ(Pd–Cα) donor and σ*(C_β–X) acceptor orbitals, respectively) fully validate the molecular orbital diagram illustrated in Figure 5, as well as the conclusions made on the basis of that fundamental knowledge. Indeed, for substituents with high energy σ* orbitals, X = H, Me, OH and F, the calculated (a) ΔE is a very large, (b) $E^{(2)}_{ij}$ interaction energies are relatively small, and (c) $\Delta D(C_\beta–X)$ is essentially zero. These calculated parameters clearly show that the β-Pd effects via hyperconjugation for X = H, Me, OH and F are going to be relatively small. Indeed, the β-elimination barriers for these substituents are very high, $\Delta G^\ddagger_{elim}$ > 40.0 kcal/mol. Nevertheless, as expected, the importance of the β-Pd effect in these systems increases with electronegativity from left to right (β-effect follows the trend X = H < CH_3 < OH < F).[54]

However, moving down the group, the σ* orbitals of C_β–X get lower in energy for X = Cl, Br and I in that order, and the β-Pd effects are enhanced. This is observed in the decrease of energy difference, ΔE, between the Pd–C_α σ donor and C_β–X σ* acceptor orbitals. However, the energy of the orbital interaction, $E^{(2)}_{ij}$, (and the F_{ij} term) follows the trend Cl < Br > I, which is in agreement with those previously reported for substituted ethenes.[54] The trends in β-elimination barriers generally decrease as hyperconjugation increases. The slight discrepancy for X = I indicates that other factors inherent in X and its leaving group ability will also affect the elimination barrier. However, we can generally conclude that the β-Pd effect is a significant factor in lowering the β-elimination barrier.

As shown previously for Pd(II)-catalyzed C–H alkynylation with alkynyl halides (i.e., X = Br, I),[46] the β-Pd effect originates at the stage of the migratory insertion (MI) transition state **TS1** (Figure 3). Therefore, it is natural to expect the hyperconjugation to also influence the migratory insertion barrier. We previously found that the difference in reactivity between bromo- and iodo-alkynes was partially due to an increased MI barrier for X = I.[46] To gain further insight into this effect, we also computed the MI barrier ($\Delta G^\ddagger$) and reaction energy (ΔG) for X = Me relative to **1**. The calculated values for X = Me are $\Delta G^\ddagger$ = 20.9 kcal/mol and ΔG = 13.3 kcal/mol, which are 7.3 and 17.6 kcal/mol higher than those previously reported for X = Br ($\Delta G^\ddagger$ = 13.6 kcal/mol and ΔG = −4.3 kcal/mol, respectively).[46] Therefore, we would expect Pd(II)-catalyzed C–H alkynylation with a TIPS methyl alkyne substrate (i.e., with X = Me) to be impeded in two ways: i) increase in MI barrier, and ii) inability to undergo β-elimination. However, X groups with σ*(C_β–X) acceptor ability and bond strength similar to Cl and Br could be successfully employed for this or similar reactions.

To summarize, hyperconjugation is critical for the β-Pd effect in the alkenyl systems that we have studied. The hyperconjugation increases with (1) electronegativity in the order X = H ≈ CH_3 < OH < F), and (2) decreasing ΔE (i.e. energy difference between the σ (Pd–C_α) donor and σ*(C_β–X) acceptor orbitals) until it is outweighed by other factors related to electronegativity (i.e., in the order X = F > Cl > Br < I). These insights may be applied to reaction design, where the choice of an appropriate leaving group will enhance the β-Pd effect to facilitate novel reactivity.

Trends in transition metal β-effects: Impact of the transition metal. It is also expected that the β-transition metal effect is going to be heavily influenced by the identity of the participating transition metal center. Therefore, we have also studied the hyperconjugation for a series of transition metals to assess some trends in the β-transition metal effect. For our purposes, we focused on the late transition metals Fe(II), Ru(II), Os(II), Co(III), Rh(III), Ir(III), Ni(II), Pd(II), Pt(II), Cu(III), Ag(III) and Au(III) because they are invoked in many organometallic transformations and catalysis. We wish to emphasize that a general and comprehensive description of the effect of the transition metals on the hyperconjugation is a complex task with several complicating variables. These may include, but are not limited to, the nature of the auxiliary ligands and the geometrical environment of the metal centers, availability of multiple lower-lying electronic states, and electronic configurations (such as s^0d^n, s^1d^{n-1} and s^2d^{n-2}), and the tendency of metals to form various types of complexes with alkenes and alkynes, as exemplified by **2** (i.e., “constrained” geometry or metal-π complexes) and **3** (i.e., “relaxed” geometry or free metal complexes) (Figure 6). Therefore, for the sake of simplicity, we focus on selected transition metal complexes in the closed shell singlet state in order to build a general picture for transition metal β-effects that can be extrapolated for future studies of these and other important variables.

In order to account for the differences in oxidation states of metals, we derived model systems, [M] (where the brackets denote the picolinamide ligand system), from the picolinamide substrate studied for Pd(II) as shown in Figure 6. Although the computationally located structures depend on the nature of the transition metal, below we discuss only the most energetically favorable complexes in the closed shell singlet state. It is our anticipation that such an approach will provide a consistent picture. The calculated hyperconjugation parameters and the free energy barriers for β-bromide elimination for these are provided in Table 3. With some exceptions, we generally find that **2** and **3** give consistent results and lead to the same conclusions. (See the example with M = Pd(II) above and the Supporting Information for the full dataset.)

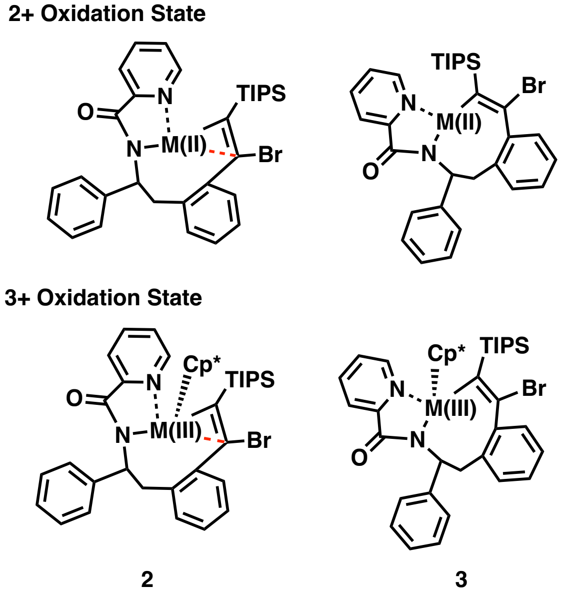

Figure 6. Model complexes used to compute hyperconjugation parameters with different transition metals. Transition metals in the 2+ oxidation state are as is and those in the 3+ oxidation state have an additional pentamethylcyclopentadienyl (Cp*) ligand.

A few general observations emerge from the dataset. We observe strong σ donating ability of the [M]–C_α bonds with $E^{(2)}_{ij} > 18.9$ kcal/mol. This is consistent with significant elongation of the C_β–Br bond in the range of 0.06-0.21 Å. The calculated trends in the hyperconjugation parameters are consistent with the electronegativities of the studied ions, which roughly fall within the range of 1.4–1.8.[59] In general, trends in the calculated $E^{(2)}_{ij}$ and $\Delta D(C_\beta\text{–Br})$ values correlate with the free energy barriers for β-bromide elimination, which are very low, $\Delta G^{\ddagger}_{\text{elim}} < 5.6$ kcal/mol. This is an indication of the generality of transition metal β-effects for the studied metals and suggests that this effect may be more prevalent than has been appreciated. Au(III) has the lowest combination of $E^{(2)}_{ij}$ and $\Delta D(C_\beta\text{–Br})$ values that we computed, and likewise its $\Delta G^{\ddagger}_{\text{elim}}$ is the highest (8.7 kcal/mol).

Close analysis of these data show that upon going down a group (i.e., in going from the first-row metals to the third-row metals), the $E^{(2)}_{ij}$ and $\Delta D(C_\beta\text{–Br})$ parameters decrease, and consistently the free energy barriers for β-bromide elimination increase. Thus, in general, it can be predicted that first row transition metals will exhibit the strongest hyperconjugative interactions and therefore the strongest β-effects.

Table 2. Hyperconjugation parameters for Pd-alkenyl intermediate **3** with different [M] substituents, where the brackets denote the picolinamide ligand system.

[M], where M =	Str.	$\Delta D(C_\beta\text{–Br})$ Å	$E^{(2)}_{ij}$ kcal/mol	ΔE au	$\Delta G^{\ddagger}_{\text{elim}}$ kcal/mol
Fe(II)	**2**	0.19	58.6	0.29	0.2
Ru(II)	**2**	0.15	43.6	0.33	0.4
Os(II)	**2**	0.06	25.7	0.43	3.9
Ni(II)	**3**	0.15	38.3	0.32	0.7
Pd(II)	**3**	0.10	28.5	0.36	3.6
Pt(II)	**3**	0.09	20.2	0.44	5.6
Co(III)	**3**	0.21	32.4	0.33	−0.5
Rh(III)	**3**	0.20	29.0	0.35	0.6
Ir(III)	**3**	0.15	21.5	0.42	2.3
Cu(III)	**3**	0.16	37.5	0.29	−0.4
Ag(III)	**3**	0.16	39.9	0.27	0.3
Au(III)	**3**	0.07	18.9	0.45	8.7

Moving along the period of the transition metal series does not provide a clear trend but does indicate that early metals exhibit stronger hyperconjugative interactions. However, in the data, we see various anomalies. For example, careful inspection of the geometric and NBO data for the Rh(III) case suggest that the C_β–Br bond is also activated by donation from the Cp* ligand and which changes the geometry around the Rh(III) center and consequently, hyperconjugation parameters. This reiterates the importance of ligand environment and molecular geometry on stereoelectronic effects in transition metal complexes. Regardless, it is likely that trends for σ-donating ability of [M]–C_α bonds within the periodic rows follow electronegativity, but that the results are very sensitive to electron count and the ligand environment.

Conclusions

We provide a comprehensive theoretical and historical context for the β-effects of transition metal ions, in particular Pd(II). We found that Pd(II) imparts a stronger β-effect than Si to stabilize a cation through hyperconjugation (σπ conjugation,) or in stabilizing the transition state for a departing nucleofuge (σσ conjugation). Due to the established connection between these modes of hyperconjugation, we are able to focus on one (σσ conjugation) to study the strength and generality of transition metal β-effects in an experimentally relevant system.

We established convenient and practical computational parameters to investigate the hyperconjugation for various X substituents on C_β–center and transition metals: (a) the degree elongation of C_β–X bond, i.e. $\Delta D(C_\beta–X)$, relative to a reference with baseline levels of hyperconjugation (i.e., [M] = H for a given system); (b) the second-order perturbation energy, $E^{(2)}_{ij}$, extracted from the NBO analysis, that measures the interaction energy between the occupied $\sigma([M]–C_\alpha)$ and the empty $\sigma^*(C_\beta–X)$ orbitals; (c) the energy gap between these orbitals, ΔE; and (d) the free energy barrier for β-elimination of the X group, $\Delta G^{\ddagger}_{elim}$.

We have shown that the nature of a substituent (X) on C_β critically affects the σσ conjugation and, consequently, the energy barrier to vinyl β-elimination. We find that the β-Pd effect is relatively small for X = H, Me, OH and F, but significant for X = Cl, Br and I.

We subsequently investigated β-effects (via σσ conjugation) in *N,N*-picolinamide vinyl metalacycles with β-substituents, [M], of other transition metals, such as M = Fe(II), Ru(II), Os(II), Co(III), Rh(III), Ir(III), Ni(II), Pd(II), Pt(II), Cu(III), Ag(III), and Au(III). All of the metals studied have exceptional $[M]–C_\alpha$ σ-donating ability and facilitate rapid vinyl β-bromide elimination. Interestingly, the first-row transition metals exhibit the strongest β-effects. Electronegativity is an adequate guide for predicting relative $[M]–C_\alpha$ σ-donating ability, but with the caveat that the β-effects appear to be highly sensitive to ligand environment, d-electron count and molecular geometry.

These findings lead us to propose that transition metal β-effects may be more common than previously appreciated. The presented results provide a foundation: (a) to build a better theoretical understanding of the factors that may affect transition metal β-effects, such as specific metal-ligand interactions and electronic states of catalyst, and (b) to invoking transition metal β-effects in the reaction design. Specifically, the choice of an appropriate leaving group (X) and transition metal could facilitate novel reactivity with different types of catalysts.

Computational Details

The Gaussian 09 suite of programs[60] was used for all calculations. Geometry optimizations and frequency calculations for all reported structures were performed at the B3LYP-D3BJ/BS1 level of theory, where BS1 = Lanl2dz for Cl, Br, I, Fe, Ru, Os, Ni, Pd, Pt, Co, Rh, Ir, Cu, Ag, Au with the corresponding Hay-Wadt effective core potentials (ECP) and 6-31G(d,p) for all other atoms. Grimme's empirical dispersion-correction with Becke-Johnson damping was used for B3LYP.[61] Each reported minimum has zero imaginary frequencies and each transition state (TS) structure has only one imaginary frequency. Intrinsic reaction coordinate (IRC) calculations were performed for transition state structures to confirm their identity.

Model system calculations (**A**-**C**) were optimized in the gas phase. These energies are reported in the text. Singlet point energies computed using the self-consistent reaction field polarizable continuum model (IEF-PCM)[62-64] with dichloromethane as the solvent as well as at the B3LYP-D3BJ/BS2, where BS2 = Def2-TZVPD, and CCSD(T)/BS1 levels of theory are reported in the Supporting Information. All other energies in the text (**2**, **3**, etc.) are calculated for structures optimized with the solvation model at the B3LYP-D3BJ/BS1 level of theory.

Natural bond orbital (NBO) analysis[65-66] was performed for selected structures using the NBO program (version 3.1)[67], as implemented in G09. Donor-acceptor interactions are analyzed with the second-order perturbation of the natural bond orbitals. This analysis provides a quantitative measure ($E^{(2)}_{ij}$) of the interaction between an occupied donor NBO (*i*) and an empty acceptor NBO (*j*).[54]

ASSOCIATED CONTENT

Supporting Information. Computational details, Energies and frequency analysis, Cartesian coordinates of all reported structures. This material is available free of charge via the Internet at http://pubs.acs.org

AUTHOR INFORMATION

Corresponding Authors
dmusaev@emory.edu

NOTES

The authors declare no competing financial interests.

ACKNOWLEDGMENT

This work was supported by the National Science Foundation under the CCI Center for Selective C–H Functionalization (CHE-1700982). D.G.M. gratefully acknowledges the NSF MRI-R2 grant (CHE-0958205) and the use of the resources of the Cherry Emerson Center for Scientific Computation at Emory University.

REFERENCES

1. Alabugin, I. V. *Stereoelectronic Effects: A Bridge between Structure and Reactivity*. John Wiley & Sons, Ltd.: Chichester, UK, 2016.
2. Alabugin, I. V.; Gilmore, K. M.; Peterson, P. W. Hyperconjugation. *Wires Comput. Mol. Sci.* **2011**, *1*, 109-141.
3. Vatsadze, S. Z.; Loginova, Y. D.; Dos Passos Gomes, G.; Alabugin, I. V. Stereoelectronic Chameleons: The Donor-Acceptor Dichotomy of Functional Groups. *Chem. Eur. J.* **2017**, *23*, 3225-3245.
4. Creary, X.; Kochly, E. D. Systematic Repression of Beta-Silyl Carbocation Stabilization. *J. Org. Chem.* **2009**, *74*, 7210-7210.
5. Davis, D. D.; Jacocks, H. M. Deoxymetalation Reactions - the Mechanisms of Deoxysilylation of Mono-Trimethylsilyl-Substituted and Bis-Trimethylsilyl-Substituted Alcohols and a Comparison to the Mechanism of Deoxystannylation and Deoxyplumbylation. *J. Organomet. Chem.* **1981**, *206*, 33-47.
6. Gabelica, V.; Kresge, A. J. Protonation of Trimethylsilyl-Substituted Carbon-Carbon Multiple Bonds in Aliphatic Systems. Conformational Dependence of the Beta-Silyl Stabilization of Carbocations. *J. Am. Chem. Soc.* **1996**, *118*, 3838-3841.
7. Lambert, J. B.; Wang, G. T.; Finzel, R. B.; Teramura, D. H. Stabilization of Positive Charge by Beta-Silicon. *J. Am. Chem. Soc.* **1987**, *109*, 7838-7845.
8. Apeloig, Y.; Arad, D. Stabilization of the Phenyl Cation by Hyperconjugation. *J. Am. Chem. Soc.* **1985**, *107*, 5285-5286.
9. Himeshima, Y.; Kobayashi, H.; Sonoda, T. A 1st Example of Generating Aryl Cations in the Solvolysis of Aryl Triflates in Trifluoroethanol. *J. Am. Chem. Soc.* **1985**, *107*, 5286-5288.
10. Garlets, Z. J.; Davies, H. M. L. Harnessing the Beta-Silicon Effect for Regioselective and Stereoselective Rhodium(II)-Catalyzed C-H Functionalization by Donor/Acceptor Carbenes Derived from 1-Sulfonyl-1,2,3-Triazoles. *Org. Lett.* **2018**, *20*, 2168-2171.
11. Chiavarino, B.; Crestoni, M. E.; Fornarini, S. Radiolytic Silylation of Alkenes and Alkynes by Gaseous R_3Si+ Ions. Stereochemical Evidence for the Beta-Silyl Effect. *J. Am. Chem. Soc.* **1998**, *120*, 1523-1527.
12. Commandeur, C.; Thorimbert, S.; Malacria, M. Chemo- and Stereoselective Palladium-Catalyzed Allylic Alkylations Controlled by Silicon. *J. Org. Chem.* **2003**, *68*, 5588-5592.
13. Olofsson, K.; Larhed, M.; Hallberg, A. Highly Regioselective Palladium-Catalyzed Internal Arylation of Allyltrimethylsilane with Aryl Triflates. *J. Org. Chem.* **1998**, *63*, 5076-5079.
14. Duttwyler, S.; Zhang, Y.; Linden, A.; Reed, C. A.; Baldridge, K. K.; Siegel, J. S. Synthesis and Crystal Structure of a Silyl-Stabilized Allyl Cation Formed by Disruption of an Arene by a Protonation-Hydrosilylation Sequence. *Angew. Chem., Int. Ed.* **2009**, *48*, 3787-3790.
15. Lambert, J. B.; Liu, C. Q.; Kouliev, T. A Stable Beta-Silyl Carbocation with Allyl Conjugation. *J. Phys. Org. Chem.* **2002**, *15*, 667-671.
16. Klaer, A.; Saak, W.; Haase, D.; Muller, T. Molecular Structure of a Cyclopropyl Substituted Vinyl Cation. *J. Am. Chem. Soc.* **2008**, *130*, 14956-14957.
17. Lambert, J. B.; Zhao, Y. A Stable Beta-Silyl Carbocation. *J. Am. Chem. Soc.* **1996**, *118*, 7867-7868.
18. Hassall, K. S.; White, J. M. Solution and X-Ray Structure of Triethylsilylmethyl-Substituted Tropylium Cation. *Org. Lett.* **2004**, *6*, 1737-1739.
19. Creary, X.; Butchko, M. A. Beta-Trimethylsilyl Cyclopropylcarbenes. *J. Org. Chem.* **2001**, *66*, 1115-1121.
20. Creary, X.; Butchko, M. A. Beta-Silylcarbenes from Isolable Diazosilanes. *J. Org. Chem.* **2002**, *67*, 112-118.
21. Lambert, J. B. The Interaction of Silicon with Positively Charged Carbon. *Tetrahedron* **1990**, *46*, 2677-2689.
22. Lambert, J. B.; Zhao, Y.; Emblidge, R. W.; Salvador, L. A.; Liu, X. Y.; So, J. H.; Chelius, E. C. The Beta Effect of Silicon and Related Manifestations of Sigma Conjugation. *Acc. Chem. Res.* **1999**, *32*, 183-190.
23. White, J. M.; Clark, C. I. Stereoelectronic Effects of the Group 4 Metal Substituents in Organic Chemistry. In *Topics in Stereochemistry*, Denmark, S. E., Ed. Wiley: New York, 2007; Vol. 22.
24. Traylor, T. G.; Hanstein, W.; Berwin, H. J.; Clinton, N. A.; Brown, R. S. Vertical Stabilization of Cations by Neighboring Sigma-Bonds - General Considerations. *J. Am. Chem. Soc.* **1971**, *93*, 5715-5725.
25. Traylor, T. G.; Berwin, H. J.; Jerkuncia, J.; Hall, M. L. Sigma-pi Conjugation: Occurence and Magnitude. *Pure Appl. Chem.* **1972**, *30*, 599-606.
26. Stewart, P. S.; Chen, M.; Roush, W. R.; Ess, D. H. Thermodynamic Control of 1,3-Boratropic Shifts of alpha- and gamma-Stannyl-Substituted Allylboranes: Hyperconjugation Outweighs Steric Effects. *Org. Lett.* **2011**, *13*, 1478-1481.

27. Chan, V. Y.; Clark, C. I.; Giordano, J.; Green, A. J.; Karalis, A.; White, J. M. Ground-State Stereoelectronic Effects Involving Silicon and Germanium: A Comparison of the Effects of Germanium and Silicon Substituents on C-O Bond Lengths at the Beta-Position. *J. Org. Chem.* **1996**, *61*, 5227-5233.

28. Green, A. J.; Kuan, Y. L.; White, J. M. Ground-State Stereoelectronic Effects of Silicon - a Comparison of the Effects of Synperiplanar and Antiperiplanar Silicon on C-O Bond Lengths at the Beta-Position. *J. Org. Chem.* **1995**, *60*, 2734-2738.

29. White, J. M.; Robertson, G. B. Stereoelectronic Effect of the Trimethylsilyl Substituent Upon C-O Bond Lengths at the Beta-Position - Some Structural Studies. *J. Org. Chem.* **1992**, *57*, 4638-4644.

30. Kuan, Y. L.; White, J. M. Conformational-Analysis of T-5-Methyl-T-2-(Trimethylsilyl)Cyclohexan-R-Ol and Its Derived Esters. *J. Chem. Soc., Chem. Commun.* **1994**, 1195-1196.

31. Spiniello, M.; White, J. A. Structural Investigations into the Beta-Effect of Pentavalent Silicon. *Organometallics* **2008**, *27*, 994-999.

32. White, J. M. Reactivity and Ground-State Effects of Silicon in Organic-Chemistry. *Aust. J. Chem.* **1995**, *48*, 1227-1251.

33. Fujiyama, R.; Alam, M. A.; Shiiyama, A.; Munechika, T.; Fujio, M.; Tsuno, Y. The Beta-Silicon Effect. 4: Substituent Effects on the Solvolysis of 1-Alkyl-2-(Aryldimethylsilyl)Ethyl Trifluoroacetates. *J. Phys. Org. Chem.* **2010**, *23*, 819-827.

34. Cook, M. A.; Eaborn, C.; Walton, D. R. M. The Mechanism of Solvolysis of (2-Bromoethyl)Trimethylsilane. Evidence for the Migration of the Trimethylsilyl Group. *J. Organomet. Chem.* **1970**, *24*, 301-306.

35. Fujio, M.; Umezaki, Y.; Alam, M. A.; Kikukawa, K.; Fujiyama, R.; Tsuno, Y. The Beta-Silicon Effect. Ii. Substituent Effects on the Solvolysis of 1-Aryl-2-(Aryldimethylsilyl)Ethyl 3,5-Dinitrobenzoates. *Bull. Chem. Soc. Jpn.* **2006**, *79*, 1091-1099.

36. Fujio, M.; Uchida, M.; Okada, A.; Alam, M. A.; Fujiyama, R.; Siehl, H. U.; Tsuno, Y. The Yukawa-Tsuno Relationship Tor the Beta-Silicon Effect in the Solvolysis Rates of 2-(Aryldimethylsily)Ethyl Chlorides. *Bull. Chem. Soc. Jpn.* **2005**, *78*, 1834-1842.

37. Brook, M. A.; Neuy, A. The Beta-Effect - Changing the Ligands on Silicon. *J. Org. Chem.* **1990**, *55*, 3609-3616.

38. Sugawara, M.; Yoshida, J. Remarkable Gamma-Effect of Tin: Acid-Promoted Cyclopropanation Reactions of Alpha-((Alkoxycarbonyl)Oxy)Stannanes with Alkenes. *J. Am. Chem. Soc.* **1997**, *119*, 11986-11987.

39. Sugawara, M.; Yoshida, J. Evaluation of Beta- and Gamma-Effects of Group 14 Elements Using Intramolecular Competition. *J. Org. Chem.* **2000**, *65*, 3135-3142.

40. Apeloig, Y.; Schleyer, P. V.; Pople, J. A. Molecular-Orbital Theory of Electronic-Structure of Molecules .35. Beta-Substituent Effects on Stabilities of Ethyl and Vinyl Cations - Comparison with Isoelectronic Methyl Boranes - Relative Importance of Hyperconjugative and Inductive Effect. *J. Am. Chem. Soc.* **1977**, *99*, 5901-5909.

41. White, J. C.; Cave, R. J.; Davidson, E. R. An ab initio Investigation of the Stabilization of Selected Beta-Substituted Ethyl Cations and Alpha-Substituted Methyl Cations. *J. Am. Chem. Soc.* **1988**, *110*, 6308-6314.

42. Alabugin, I. V.; Manoharan, M. Effect of Double-Hyperconjugation on the Apparent Donor Ability of sigma-Bonds: Insights from the Relative Stability of delta-Substituted Cyclohexyl Cations. *J. Org. Chem.* **2004**, *69*, 9011-9024.

43. Lambert, J. B.; Zhao, Y. Beta Effect of Phosphorus Functionalities. *J. Am. Chem. Soc.* **1996**, *118*, 3156-3167.

44. Lambert, J. B.; Beadle, B. M.; Kuang, K. Y. Phenylsulfonyl as a Beta Participating Group. *J. Org. Chem.* **1999**, *64*, 9241-9246.

45. Viart, H. M. F.; Bachmann, A.; Kayitare, W.; Sarpong, R. Beta-Carboline Amides as Intrinsic Directing Groups for C(sp^2)-H Functionalization. *J. Am. Chem. Soc.* **2017**, *139*, 1325-1329.

46. Usui, K.; Haines, B. E.; Musaev, D. G.; Sarpong, R. Understanding Regiodivergence in a Pd(II)-Mediated Site-Selective C–H Alkynylation. *ACS Catal.* **2018**, *8*, 4516-4527.

47. dos Passos Gomes, G.; Alabugin, I. V. Drawing Catalytic Power from Charge Separation: Stereoelectronic and Zwitterionic Assistance in the Au(I)-Catalyzed Bergman Cyclization. *J. Am. Chem. Soc.* **2017**, *139*, 3406-3416.

48. Seyferth, D.; Williams, G. H.; Traficante, D. D. Organocobalt Cluster Complexes .13. Nuclear Magnetic-Resonance Spectroscopic Evidence Concerning Stabilization of (Nonacarbonyltricobalt)Carbon Substituted Carbonium-Ions. *J. Am. Chem. Soc.* **1974**, *96*, 604-606.

49. Harrington, L. E.; Vargas-Baca, I.; Reginato, N.; McGlinchey, M. J. Spectroscopic and Computational Assessment of the Rotational Barrier of a Ferrocenyl-Stabilized Cyclopentadienyl Cation: Evidence for the First Hydroxyfulvalene Ligand. *Organometallics* **2003**, *22*, 663-669.

50. Lambert, J. B.; Emblidge, R. W. Nucleophilic Catalysis in Deoxymercuration: The Beta Effect of Mercury. *J. Phys. Org. Chem.* **1993**, *6*, 555-560.

51. Ibrahim, M. R.; Jorgensen, W. L. Ab initio Investigations of the Beta-Silicon Effect on Alkyl and

Cyclopropyl Carbenium Ions and Radicals. *J. Am. Chem. Soc.* **1989**, *111*, 819-824.

52. Nguyen, K. A.; Gordon, M. S.; Wang, G. T.; Lambert, J. B. Stabilization of Beta-Positive Charge by Silicon, Germanium, or Tin. *Organometallics* **1991**, *10*, 2798-2803.

53. Wierschke, S. G.; Chandrasekhar, J.; Jorgensen, W. L. Magnitude and Origin of the Beta-Silicon Effect on Carbenium Ions. *J. Am. Chem. Soc.* **1985**, *107*, 1496-1500.

54. Alabugin, I. V.; Zeidan, T. A. Stereoelectronic Effects and General Trends in Hyperconjugative Acceptor Ability of Sigma Bonds. *J. Am. Chem. Soc.* **2002**, *124*, 3175-3185.

55. NBO analysis is not effective for quantification of the hyperconjugation in carbocation structure A because the program locates the double bonded structure as the optimal Lewis structure.

56. Cera, G.; Haven, T.; Ackermann, L. Iron-Catalyzed C-H Alkynylation through Triazole Assistance: Expedient Access to Bioactive Heterocycles. *Chem. Eur. J.* **2017**, *23*, 3577-3582.

57. Ruan, Z. X.; Sauermann, N.; Manoni, E.; Ackermann, L. Manganese-Catalyzed C-H Alkynylation: Expedient Peptide Synthesis and Modification. *Angew. Chem., Int. Ed.* **2017**, *56*, 3172-3176.

58. Tan, E.; Konovalov, A. I.; Fernandez, G. A.; Dorel, R.; Echavarren, A. M. Ruthenium-Catalyzed Peri- and Ortho-Alkynylation with Bromoalkynes Via Insertion and Elimination. *Org. Lett.* **2017**, *19*, 5561-5564.

59. Li, K. Y.; Xue, D. F. Estimation of Electronegativity Values of Elements in Different Valence States. *J. Phys. Chem. A* **2006**, *110*, 11332-11337.

60. Gaussian 09, Revision E.01, Frisch, M. J.; Trucks, G. W.; Schlegel, H. B.; Scuseria, G. E.; Robb, M. A.; Cheeseman, J. R.; Scalmani, G.; Barone, V.; Mennucci, B.; Petersson, G. A.; Nakatsuji, H.; Caricato, M.; Li, X.; Hratchian, H. P.; Izmaylov, A. F.; Bloino, J.; Zheng, G.; Sonnenberg, J. L.; Hada, M.; Ehara, M.; Toyota, K.; Fukuda, R.; Hasegawa, J.; Ishida, M.; Nakajima, T.; Honda, Y.; Kitao, O.; Nakai, H.; Vreven, T.; Montgomery, J. A., Jr.; Peralta, J. E.; Ogliaro, F.; Bearpark, M.; Heyd, J. J.; Brothers, E.; Kudin, K. N.; Staroverov, V. N.; Kobayashi, R.; Normand, J.; Raghavachari, K.; Rendell, A.; Burant, J. C.; Iyengar, S. S.; Tomasi, J.; Cossi, M.; Rega, N.; Millam, M. J.; Klene, M.; Knox, J. E.; Cross, J. B.; Bakken, V.; Adamo, C.; Jaramillo, J.; Gomperts, R.; Stratmann, R. E.; Yazyev, O.; Austin, A. J.; Cammi, R.; Pomelli, C.; Ochterski, J. W.; Martin, R. L.; Morokuma, K.; Zakrzewski, V. G.; Voth, G. A.; Salvador, P.; Dannenberg, J. J.; Dapprich, S.; Daniels, A. D.; Farkas, Ö.; Foresman, J. B.; Ortiz, J. V.; Cioslowski, J.; Fox, D. J. Gaussian, Inc., Wallingford CT, 2009.

61. Grimme, S.; Ehrlich, S.; Goerigk, L. Effect of the Damping Function in Dispersion Corrected Density Functional Theory. *J. Comput. Chem.* **2011**, *32*, 1456-1465.

62. Cances, E.; Mennucci, B.; Tomasi, J. A New Integral Equation Formalism for the Polarizable Continuum Model: Theoretical Background and Applications to Isotropic and Anisotropic Dielectrics. *J. Chem. Phys.* **1997**, *107*, 3032-3041.

63. Mennucci, B.; Tomasi, J. Continuum Solvation Models: A New Approach to the Problem of Solute's Charge Distribution and Cavity Boundaries. *J. Chem. Phys.* **1997**, *106*, 5151-5158.

64. Scalmani, G.; Frisch, M. J. Continuous Surface Charge Polarizable Continuum Models of Solvation. I. General Formalism. *J. Chem. Phys.* **2010**, *132*, 114110-114124.

65. Reed, A. E.; Weinhold, F. Natural Localized Molecular-Orbitals. *J. Chem. Phys.* **1985**, *83*, 1736-1740.

66. Reed, A. E.; Weinstock, R. B.; Weinhold, F. Natural-Population Analysis. *J. Chem. Phys.* **1985**, *83*, 735-746.

67. Glendening, E. D.; Reed, A. E.; Carpenter, J. E.; Weinhold, F. NBO, version 3.1; University of Wisconsin: Madison, WI, 1996.

Table of Contents

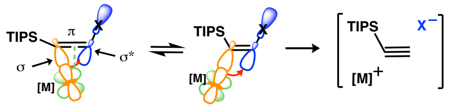

X = H, Me, OH, F, Cl, Br, I
M = Fe, Ru, Os, Pd, Ni, Pt, Co, Rh, Ir, Cu, Ag, Au